University Library

A gateway to Melbourne's research publications

Minerva Access is the Institutional Repository of The University of Melbourne

Author/s:
Koutsakos, M;Lee, WS;Reynaldi, A;Tan, HX;Gare, G;Kinsella, P;Liew, KC;Taiaroa, G;Williamson, DA;Kent, HE;Stadler, E;Cromer, D;Khoury, DS;Wheatley, AK;Juno, JA;Davenport, MP;Kent, SJ

Title:
The magnitude and timing of recalled immunity after breakthrough infection is shaped by SARS-CoV-2 variants

Date:
2022-07-12

Citation:
Koutsakos, M., Lee, W. S., Reynaldi, A., Tan, H. X., Gare, G., Kinsella, P., Liew, K. C., Taiaroa, G., Williamson, D. A., Kent, H. E., Stadler, E., Cromer, D., Khoury, D. S., Wheatley, A. K., Juno, J. A., Davenport, M. P. & Kent, S. J. (2022). The magnitude and timing of recalled immunity after breakthrough infection is shaped by SARS-CoV-2 variants. Immunity, 55 (7), pp.1316-1326.e4. https://doi.org/10.1016/j.immuni.2022.05.018.

Persistent Link:
https://hdl.handle.net/11343/325670

Since January 2020 Elsevier has created a COVID-19 resource centre with free information in English and Mandarin on the novel coronavirus COVID-19. The COVID-19 resource centre is hosted on Elsevier Connect, the company's public news and information website.

Elsevier hereby grants permission to make all its COVID-19-related research that is available on the COVID-19 resource centre - including this research content - immediately available in PubMed Central and other publicly funded repositories, such as the WHO COVID database with rights for unrestricted research re-use and analyses in any form or by any means with acknowledgement of the original source. These permissions are granted for free by Elsevier for as long as the COVID-19 resource centre remains active.

Article

Immunity

The magnitude and timing of recalled immunity after breakthrough infection is shaped by SARS-CoV-2 variants

Graphical abstract

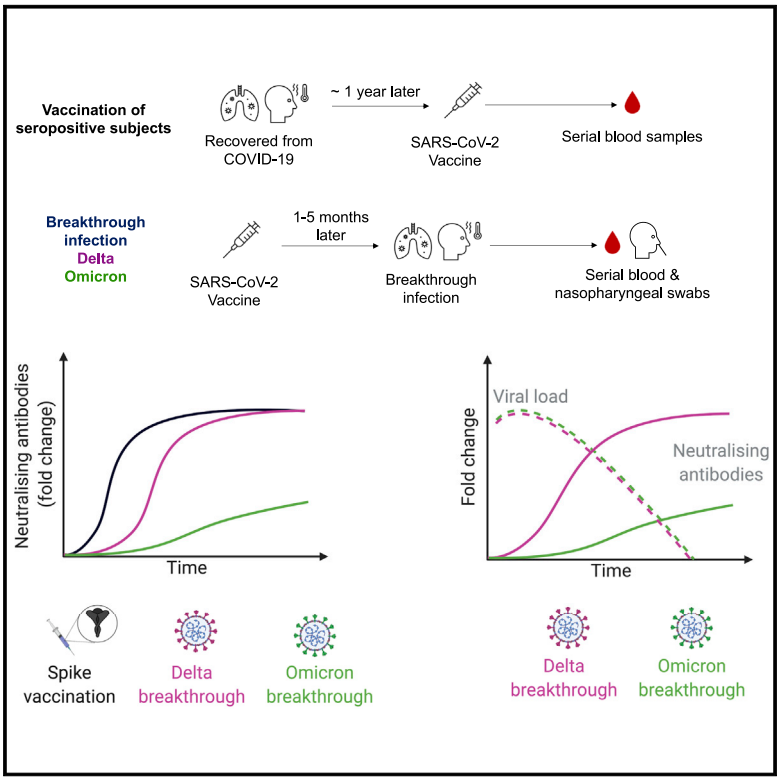

Highlights

- Vaccination of seropositive people elicits robust recall of spike-specific immunity
- Immune recall following breakthrough infection is variable in timing and magnitude
- Antibody recall during Delta breakthrough infection coincides with viral clearance
- Omicron breakthrough infection elicits less extensive immune recall compared with Delta

Authors

Marios Koutsakos, Wen Shi Lee, Arnold Reynaldi, ..., Jennifer A. Juno, Miles P. Davenport, Stephen J. Kent

Correspondence

a.wheatley@unimelb.edu.au (A.K.W.), jennifer.juno@unimelb.edu.au (J.A.J.), m.davenport@unsw.edu.au (M.P.D.), skent@unimelb.edu.au (S.J.K.)

In brief

Koutsakos et al. analyzed the recall of spike-specific immunity following vaccination of seropositive individuals and breakthrough infections in vaccinated individuals. Compared with recall following vaccination, recall during breakthrough infections is delayed and variable in magnitude. The recall of neutralizing antibodies temporally correlated with control of Delta breakthrough infection viral load, while Omicron breakthrough elicited less extensive immune recall versus Delta.

Koutsakos et al., 2022, Immunity *55*, 1316–1326
July 12, 2022 © 2022 Elsevier Inc.
https://doi.org/10.1016/j.immuni.2022.05.018

CellPress

CellPress

Immunity

Article

The magnitude and timing of recalled immunity after breakthrough infection is shaped by SARS-CoV-2 variants

Marios Koutsakos,[1,6] Wen Shi Lee,[1,6] Arnold Reynaldi,[2] Hyon-Xhi Tan,[1] Grace Gare,[1] Paul Kinsella,[3] Kwee Chin Liew,[3] George Taiaroa,[3] Deborah A. Williamson,[3,4] Helen E. Kent,[1] Eva Stadler,[2] Deborah Cromer,[2] David S. Khoury,[2] Adam K. Wheatley,[1,*] Jennifer A. Juno,[1,*] Miles P. Davenport,[2,*] and Stephen J. Kent[1,5,7,*]

[1]Department of Microbiology and Immunology, University of Melbourne, Peter Doherty Institute for Infection and Immunity, Melbourne, VIC, Australia

[2]Kirby Institute, University of New South Wales, Kensington, NSW, Australia

[3]Victorian Infectious Diseases Reference Laboratory, The Royal Melbourne Hospital at The Peter Doherty Institute for Infection and Immunity, Melbourne, VIC, Australia

[4]Department of Infectious Diseases, The University of Melbourne at the Peter Doherty Institute for Infection and Immunity, Melbourne, VIC 3000, Australia

[5]Melbourne Sexual Health Centre and Department of Infectious Diseases, Alfred Hospital and Central Clinical School, Monash University, Melbourne, VIC, Australia

[6]These authors contributed equally

[7]Lead contact

*Correspondence: a.wheatley@unimelb.edu.au (A.K.W.), jennifer.juno@unimelb.edu.au (J.A.J.), m.davenport@unsw.edu.au (M.P.D.), skent@unimelb.edu.au (S.J.K.)

https://doi.org/10.1016/j.immuni.2022.05.018

SUMMARY

Vaccination against SARS-CoV-2 protects from infection and improves clinical outcomes in breakthrough infections, likely reflecting residual vaccine-elicited immunity and recall of immunological memory. Here, we define the early kinetics of spike-specific humoral and cellular immunity after vaccination of seropositive individuals and after Delta or Omicron breakthrough infection in vaccinated individuals. Early longitudinal sampling revealed the timing and magnitude of recall, with the phenotypic activation of B cells preceding an increase in neutralizing antibody titers. While vaccination of seropositive individuals resulted in robust recall of humoral and T cell immunity, recall of vaccine-elicited responses was delayed and variable in magnitude during breakthrough infections and depended on the infecting variant of concern. While the delayed kinetics of immune recall provides a potential mechanism for the lack of early control of viral replication, the recall of antibodies coincided with viral clearance and likely underpins the protective effects of vaccination against severe COVID-19.

INTRODUCTION

Vaccines encoding the spike (S) antigen of SARS-CoV-2 are effective in reducing the risk of symptomatic SARS-CoV-2 infection, as well as progression to severe COVID-19 disease (Chung et al., 2021). Neutralizing antibodies are a correlate of protection (Gilbert et al., 2021; Khoury et al., 2021) and likely act to prevent infection by blocking viral attachment and entry. However, as antibody titers naturally wane (Wheatley et al., 2021a), vaccine effectiveness drops (Cromer et al., 2022) and the frequency of "breakthrough infections" among vaccinated individuals increases in the population. The emergence of antigenic variants including Beta and Omicron have highlighted the potential for viral escape from neutralizing antibody recognition, which can considerably reduce vaccine effectiveness against acquisition of SARS-CoV-2 infection (Roessler et al., 2021). Nevertheless, vaccine-elicited immunity continues to provide robust protection against severe disease outcomes, even in the face of viral variants (Tang et al., 2021). Viral growth rates and peak viral RNA load in the upper respiratory tract are similar between vaccinated and unvaccinated infected individuals during the first week of infection (Chia et al., 2022; Kissler et al., 2021; Singanayagam et al., 2022) though vaccinated individuals consistently display more rapid clearance of viral RNA than unvaccinated controls during the second week of infection (Chia et al., 2022; Kissler et al., 2021). Importantly, there is a lower probability of culturing infectious virus from respiratory samples of infected vaccinated individuals (Shamier et al., 2021). The immunological mechanisms that underpin accelerated viral clearance remain unclear. The comparable viral load within vaccinated and unvaccinated individuals in the first week of infection suggest that residual (post-vaccination, pre-infection) antibody or T cell immunity fails

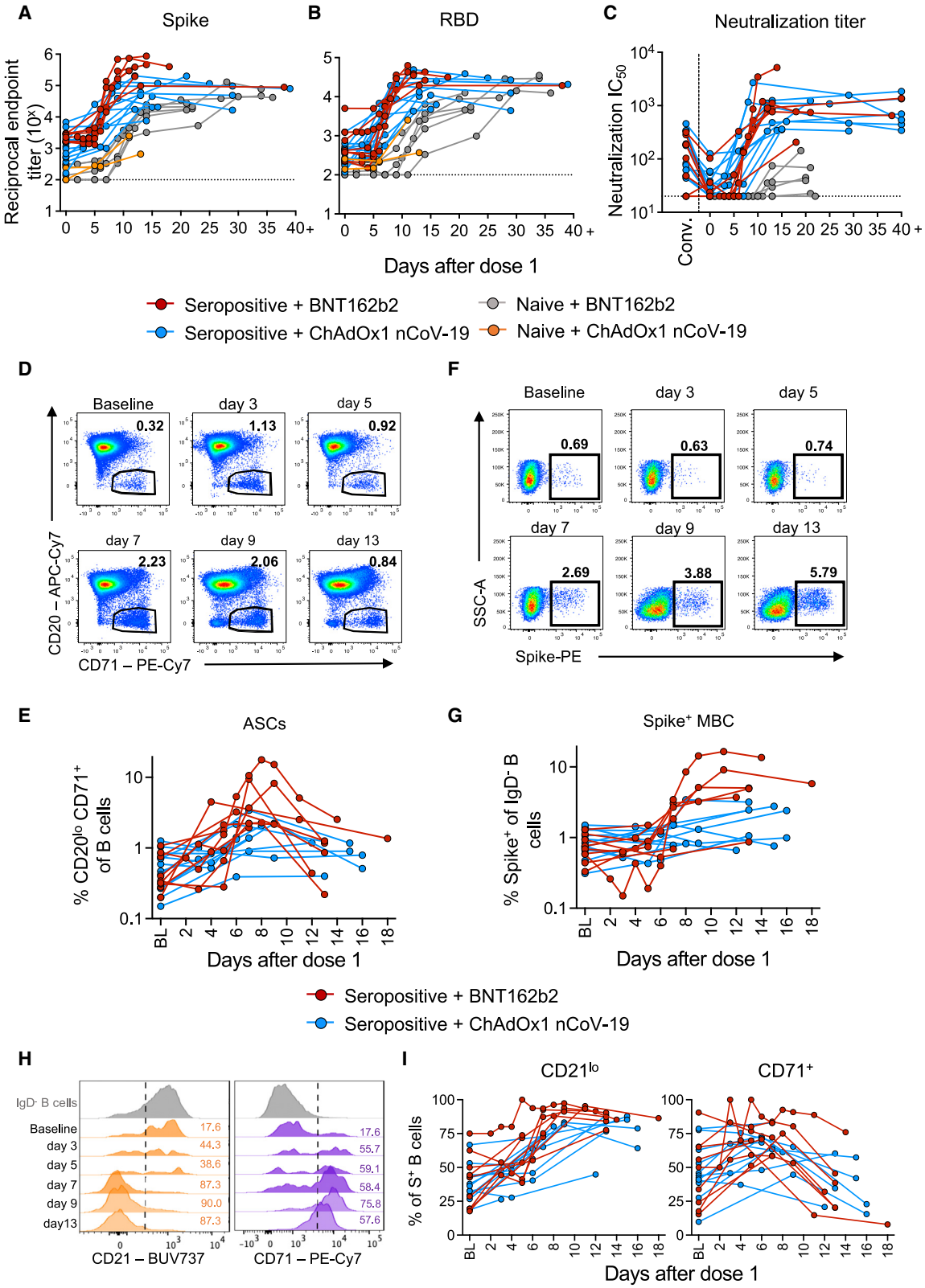

(legend on next page)

to limit early viral replication in the respiratory tract. However, the recall of SARS-CoV-2-specific antibodies, memory B and T cell responses following breakthrough infection could contribute to viral clearance and temper disease severity, as is thought to be the case for other respiratory viral infections (Ferdinands et al., 2021; Patel et al., 2021). In addition, the dynamics of immune recall are likely to be influenced by the infecting viral strain, with less cross-reactive recognition predicted for antigenically distant variants such as Omicron. Understanding the mechanisms and effectiveness of recall responses in protecting from severe SARS-CoV-2 infection is critical to informing the optimal deployment of current vaccines and guiding the design of novel vaccines to maintain maximal protection against severe disease. To date, the precise kinetics of immune recall in the context of breakthrough SARS-CoV-2 infection have not been clearly resolved. To address that, we performed thorough longitudinal sampling of seropositive individuals following vaccination, and of vaccinated individuals following breakthrough infection with Delta or Omicron variants of concern (VOCs). By analyzing the recall kinetics of S-specific humoral and cellular immunity, we found that immune recall following breakthrough infection is delayed compared with vaccination. Following breakthrough infection, peak viral load preceded the recall of S-specific antibodies, which coincided with viral clearance and likely underpins the protective effects of vaccination against severe COVID-19.

RESULTS

Spike-specific immunity is rapidly recalled following vaccination of seropositive individuals

To understand the dynamics of recall of SARS-CoV-2 spike-specific immunity, we first analyzed immune responses after vaccination of seropositive individuals. We recruited and longitudinally sampled a cohort of 25 individuals with previous PCR-confirmed SARS-CoV-2 infection and/or baseline spike protein seropositivity (seropositive group), with a comparator group of 8 seronegative individuals with no history of SARS-CoV-2 infection (naive group) (Table S1). We undertook early longitudinal sampling from day 3 onward after vaccination with either BNT162b2 or ChAdOx1 nCoV-19 vaccines. In seropositive individuals, S- and receptor binding domain (RBD)-specific antibody titers began to increase 5 days after vaccination, with titers peaking between days 10 and 14 (Figures 1A and 1B). In naive individuals, S and RBD antibody titers emerged later after the first dose (day 9 onward) and remained lower compared with immunized seropositive individuals, in line with other reports of primary immunization of immunologically naive individuals (Sahin et al., 2021). We also assessed serological responses using a live virus neutralization assay (Wheatley et al., 2021b). At the time of vaccination, only 47% of previously infected individuals had detectable plasma neutralization activity, which reflected residual activity following waning from peak neutralization titers seen in early convalescence (Figure 1C). Following the first vaccine dose, neutralizing titers increased from day 6, concomitant with the rise in S and RBD-binding antibodies, and peaked between days 10 and 14 (Figure 1C). In contrast, immunization of naive individuals elicited much lower titers of neutralizing antibodies, which only emerged around day 12 post-first dose. We applied a piecewise linear regression model to estimate the initial period of delay, the rate of increase, and fold change over baseline in the recall of antibodies (Table S2). We estimated that the initial delay phase before neutralizing antibody titers increased was 4.85 days, with a doubling time of 0.74 days thereafter and with a peak fold change over baseline of 25.8.

Memory B cells constitute an important arm of durable vaccine-elicited immunity, rapidly responding to secondary antigen exposure via differentiation into antibody-secreting cells (ASCs). To better understand memory B cell re-activation *in vivo*, we assessed changes in the frequency and phenotype of SARS-CoV-2-specific memory B cells in seropositive individuals (n = 21) in response to immunization. ASCs ($CD19^+CD20^{lo}CD71^+$, commonly termed plasmablasts) expanded in peripheral blood, increasing from as early as day 3 based on flow cytometry (estimated by piecewise linear regression modeling to occur as early as day 2.4), peaking between days 7 and 9 before contracting to near baseline frequencies from day 11 onward (Figures 1D and 1E). S-specific class-switched memory B cells ($Spike^+IgD^-CD19^+$ cells), which, unlike ASCs, constitute a stable population of quiescent memory (Wheatley et al., 2021a), were detectable in all seropositive individuals prior to vaccination (0.31%–1.5% of IgD^- B cells). Following vaccination, the frequency of S-specific class-switched B cells increased from day 7 onward based on flow cytometry (estimated as early as day 6.5) and peaked by day 10 (Figures 1F and 1G). The activation state of S-specific B cells was assessed longitudinally using surface-expressed activation markers CD21 and CD71 (Ellebedy et al., 2016). Consistent with expansion of S-specific B cells, CD21 downregulation and CD71 upregulation, both denoting cellular activation, were evident as early as day 3 and were maximal around day 9 (Figures 1H and 1I).

Given the potential of T cells to contribute to the control of viral replication and the association of $CD4^+$ T cell responses with the development of neutralizing antibodies (Koutsakos et al., 2022), we assessed the recall of S-specific $CD4^+$ and $CD8^+$ T cells following vaccination of seropositive individuals. Using re-stimulation with recombinant S protein and an activation-induced

Figure 1. Spike-specific humoral immunity is rapidly recalled following vaccination of seropositive individuals

(A–C) Serological analysis of samples following one dose of BNT162b2 or ChAdOx1 nCoV-19. Kinetics of S-specific IgG (A) and RBD-specific IgG (B) antibodies measured by ELISA and neutralizing antibodies measured by a live virus neutralization assay (C) in SARS-CoV-2 naive or seropositive individuals (seropositive N = 19, naive N = 8).

(D and E) Representative flow cytometry plots (D) and frequency (E) of antibody-secreting cells (ASCs, $CD20^{lo}CD71^+$ B cells) in SARS-CoV-2 seropositive individuals.

(F and G) Representative flow cytometry plots (F) and frequency (G) of S-specific class-switched B cells (IgD^-CD19^+) in vaccinated seropositive individuals.

(H and I) Representative flow cytometry plots (H) and frequency (I) of activation markers (CD21, CD71) within S-specific class-switched B cells (IgD^-CD19^+) in vaccinated seropositive individuals. (D–I) N = 21.

See also Figure S1.

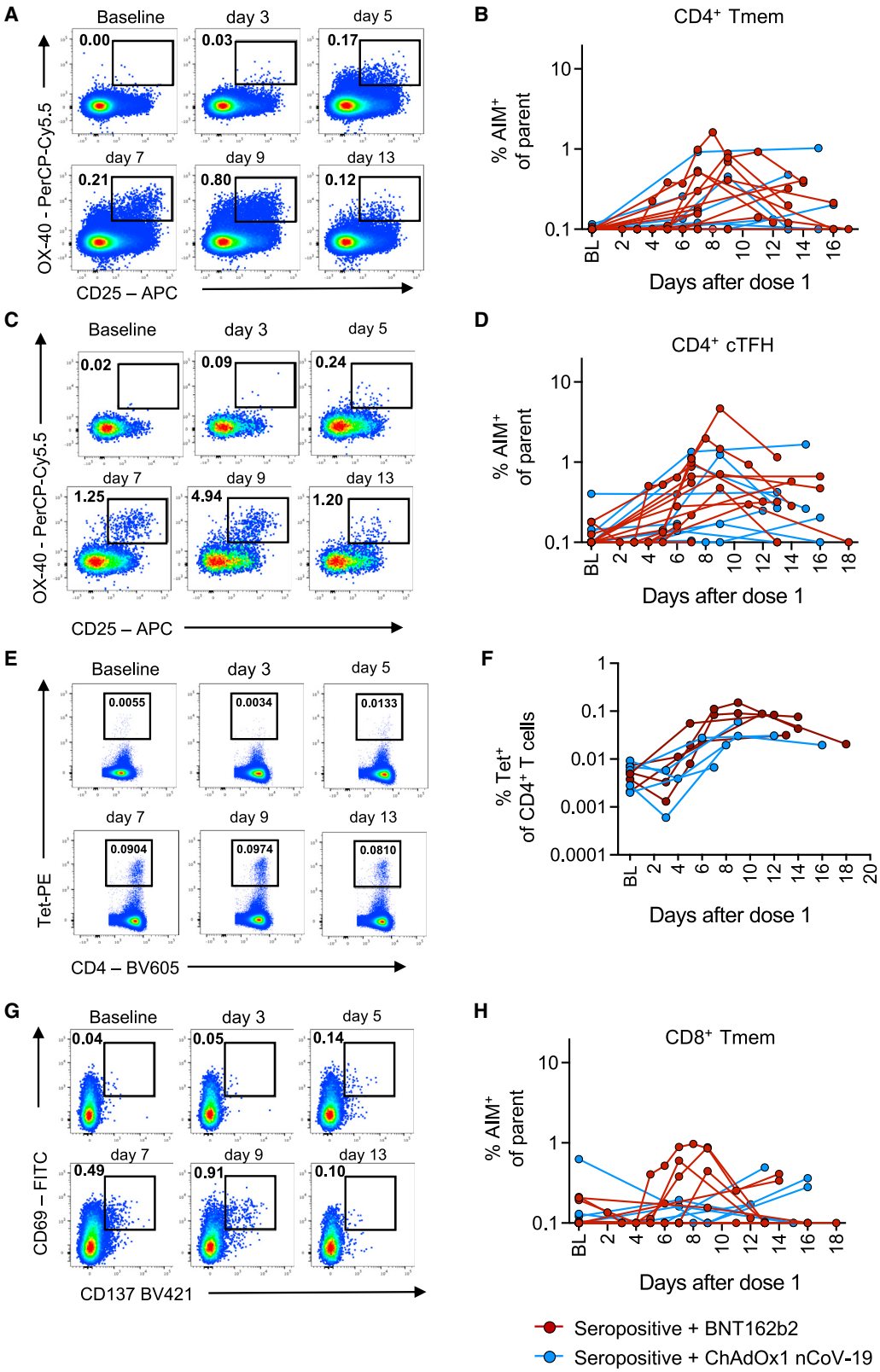

(legend on next page)

marker (AIM) assay (Figure S1), an increase in both S-specific $CD4^+$ memory T cells ($CD4^+$Tmem; $CD45RA^-CXCR5^-$) (Figures 2A and 2B) and circulating $CD4^+$ T follicular helper cells (cTFH; $CD45RA^-CXCR5^+$) was evident from day 5 onward, peaking around day 9 and declining thereafter (Figures 2C and 2D). Recall of S-specific $CD4^+$ T cell responses has also been previously reported at an epitope-specific level in a subset of the vaccination cohort (n = 10 individuals; Wragg et al., 2022). Use of an HLA-DRB1*15/S_{751} tetramer to precisely enumerate antigen-specific T cell frequencies following vaccination provided similar results to the AIM assay, with recall evident from day 5 onward and peaking between days 8 and 10 (Figures 2E and 2F). Similar kinetics were observed for S-specific $CD8^+$ memory T cells (Figures 2G and 2H), albeit at a lower magnitude than S-specific $CD4^+$ T cell responses. Using the same statistical approach as above, the initial delay for T cell recall was ~4 days (Table S2). The peak frequencies (among available samples) of ASCs and S-specific cTFH cells were positively correlated with the peak binding and neutralizing antibodies, as well as with each other (Figure S2), consistent with data from primary infection and vaccination (Koutsakos et al., 2022). Overall, vaccination of seropositive individuals led to the rapid recall of S-specific humoral and cellular immunity.

Ancestral spike-specific immunity is variably recalled following breakthrough infection of vaccinated individuals with Delta or Omicron

While vaccination of previously infected individuals provides a tractable model to assess immunological recall, the extent to which it recapitulates the dynamics of actual breakthrough infection of vaccinated individuals is unclear. Studies of the early immune kinetics of breakthrough infection are challenging, as the timing of initial infection is rarely known and is often referenced from the time of symptom onset (estimated to be a mean of 3.2 days after acquisition for Omicron and 4.3 days after acquisition for Delta) (Backer et al., 2022). Nevertheless, we recruited 16 individuals with generally mild to moderate PCR-confirmed breakthrough SARS-CoV-2 infections that occurred 1–5 months after receiving their last dose of a COVID vaccine (Table S3). Of these individuals, 8 had sequence-confirmed B.1.617.2 (Delta) infection, and 8 had B.1.1.529 (Omicron BA.1). All individuals with Delta infection and 3 of 8 individuals with Omicron infection had previously received 2 doses of a COVID-19 vaccine, while 4 individuals with an Omicron infection had received 3 doses of a COVID-19 vaccine, and 1 individual had previously recovered from COVID-19 and received 2 doses of a COVID-19 vaccine. Serial blood samples and nose swabs were obtained over 1–59 days after symptom onset, with S-specific antibody and cellular immune responses analyzed as before. We further recruited 15 individuals with indeterminate breakthrough SARS-CoV-2 infections for which one or two plasma samples were obtained between days 11 and 65 (Table S3).

We analyzed the recall of immunity established by vaccinations encoding Hu-1 spike (the ancestral strain first isolated in Wuhan), following Delta or Omicron breakthrough infection. In the context of Delta breakthrough infection (shown in purple in Figure 3), where sufficient early time point samples were available, S- and RBD-binding antibodies as well as neutralizing antibody titers remained similar to baseline for 5–7 days after symptom onset before rising during the second and third weeks (Figures 3A–3C). In contrast, during Omicron breakthrough infection (shown in green in Figure 3), recall of Hu-1 and/or Omicron cross-reactive binding and neutralizing antibodies was comparably delayed and lower in magnitude, consistent with the substantial escape from humoral immunity by Omicron (Carreño et al., 2022). Activation of vaccine-specific S-specific memory B cells, measured by CD71 upregulation or CD21 downregulation, was evident in early time points, peaking around day 10 symptom onset for both Delta and Omicron breakthrough infections and subsiding by day 30 (Figure S3A). The circulating frequencies of S-specific memory B cells peaked around day 14 for Delta breakthrough but remained largely unchanged following Omicron breakthrough (Figure 3C). ASCs expanded following both Delta and Omicron breakthrough infections and peaked around day 7 post-symptom onset. S-specific $CD4^+$ and $CD8^+$ T cell responses, as measured by AIM (Juno et al., 2020), were limited in the first 7–10 days following Delta or Omicron breakthrough infection but increased thereafter in approximately half of the donors (Figures 3E–3G). Overall, following breakthrough infection of vaccinated individuals, recall of ancestral Hu-1 S-specific immunity was variable across humoral and cellular compartments as well as across infecting VOCs.

Peak viral load precedes the recall of antibodies in breakthrough infections

To compare vaccination and breakthrough infection, we applied a piecewise linear regression model to parameterize the kinetics of immune recall. We considered the delay from exposure to symptom onset (which was known in 4 of 16 subjects and conservatively assumed this to also be 3 days in the others). The estimated time to initial increase in neutralizing and spike-binding antibody titers was longer for Omicron breakthrough infection (14.9 and 10.9 days post-exposure) compared with that of Delta breakthrough infection (7.6 and 7 days post-exposure) (Figure 4A; Table S4), both of which were delayed compared with vaccination (4.9 and 5.4 post-vaccination; Table S2). Interestingly, the time to increase in spike-specific memory B cells was not significantly different between Delta and Omicron breakthrough infections (9.9 and 10.8 respectively), though this was delayed compared with vaccination (6.5 days post-vaccination). We further stratified Delta breakthrough infections based on symptom severity, duration of symptoms or time since last vaccine dose (Figure S4; Table S4) and found no differences in time to recall of neutralizing antibodies, spike-specific

Figure 2. Spike-specific T cell immunity is rapidly recalled following vaccination of seropositive individuals

Analysis of S-specific T cells by AIM assay following one dose of BNT162b2 or ChAdOx1 nCoV-19 in SARS-CoV-2 naive or seropositive individuals.
(A–G) Representative staining and frequency of AIM markers (CD25, OX-40) on $CD4^+$ Tmem cells ($CD3^+CD4^+CD8^-CD45RA^-CXCR5^-$) (A and B) and $CD4^+$ cTFH cells ($CD3^+CD4^+CD8^-CD45RA^-CXCR5^+$) (C and D), tetramer staining (E and F) or AIM markers (CD69, CD137) on $CD8^+$ Tmem cells ($CD3^+CD8^+CD4^-$non-naive) (G and H) after stimulation with 5 μg/mL of SARS-CoV-2 S protein on different timepoints after vaccination.
See also Figures S1 and S2.

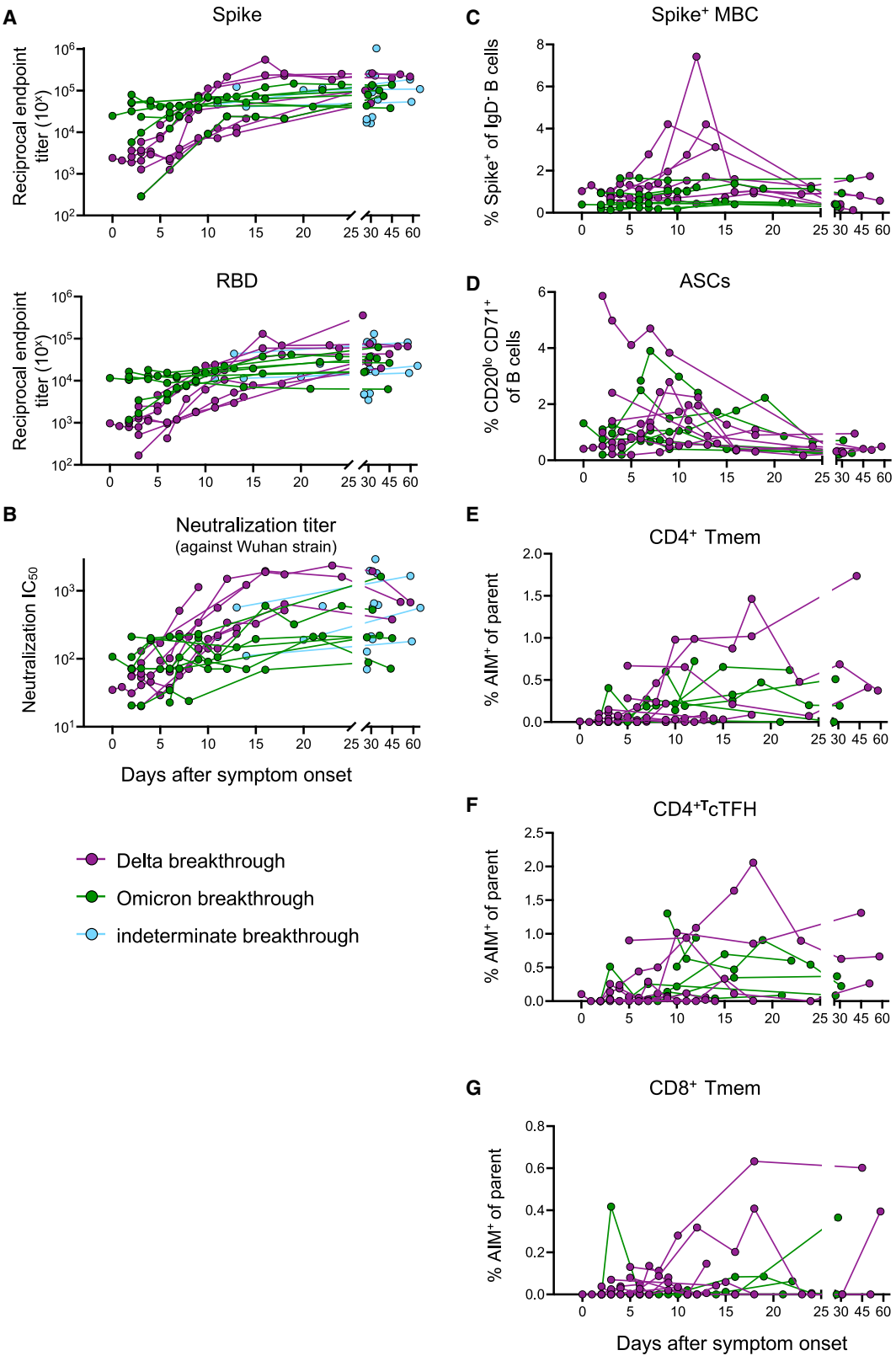

Figure 3. The recall of spike-specific humoral immunity is variable following breakthrough infection with Delta or Omicron

(A and B) (A) Kinetics of S- and RBD-specific IgG antibodies measured by ELISA and (B) of neutralizing antibodies measured by a live virus microneutralization assay. (A and B) N = 8 participants for Delta (purple), N = 8 for Omicron (green), N = 15 for indeterminate (blue).

(legend continued on next page)

IgG and spike-specific memory B cells, although our statistical power was limited due to the small sample sizes and lack of severe breakthrough infections.

To investigate the relationship between recall immunity and viral control, we analyzed viral load kinetics by qPCR of nucleocapsid (N) (Figure 4B), RNA-dependent RNA polymerase (RDRP) and S (Figures S3B and S3C) genes in serial nasopharyngeal swabs from 4 individuals with Delta and 7 individuals with Omicron breakthrough infection. This indicated a peak of viral replication (among available time points) on day 4–5 after symptom onset, followed by rapid viral clearance thereafter. Longitudinal neutralizing and binding antibody titers against the Hu-1 strain were negatively correlated with viral loads in Delta but not Omicron breakthrough infection (Figures 4C, 4D, and S3D–S3G). Comparison of viral load kinetics with the recall of antibodies indicated that the peak of viral load (day 5–6) preceded the rise in neutralizing antibodies (day 7 onward) (Figures 4E and 4F; Table S4) and that recall of humoral immunity coincided with a decrease in viral load for Delta but not Omicron breakthrough infection (Figures 4E and 4F). In summary, following breakthrough infection, immune recall of ancestral Hu-1 immunity was delayed compared with vaccination and depended on the infecting VOC, with peak viral load preceding the recall of S-specific antibodies.

DISCUSSION

Our intensive longitudinal sampling during vaccination of SARS-CoV-2 seropositive subjects and breakthrough infection revealed the sequence and dynamics of recalled immune memory to ancestral Hu-1 SARS-CoV-2 S protein. Following vaccination of subjects previously infected in 2020 with ancestral viruses (Hu-1, D614G), phenotypic activation of S-specific memory B cells coincided with the rapid expansion of ASCs (as early as day 3 after vaccination) and was followed by an increase of antigen-specific T cells in the blood (day 5 onwards). Subsequently, serological titers of both binding and neutralizing antibodies rapidly increased (day 5 onwards) and were stably maintained for at least 30 days after antigen re-exposure, with increases in frequencies of antigen-specific memory B cells following a similar trajectory. Although recall dynamics of antibody responses were relatively uniform in the context of vaccination, this was more variable in timing and magnitude during breakthrough infection of vaccinated individuals. This likely reflects the inherent heterogeneity of viral replication and timing of symptom onset between individuals, as well as the virological and antigenic differences between specific SARS-CoV-2 variants. Where the timing of exposure was more clearly defined, the delay between infection and antibody recall following Delta breakthrough infection was ~7–8 days post-exposure. In contrast, breakthrough infections with Omicron were associated with modest recall of ancestral Hu-1 spike immunity, and where detectable, rises in neutralizing responses were delayed relative to Delta by 7 days and binding antibodies by 4 days. The longer delay in recall of immunity following infection compared with vaccination may reflect differences in antigen accumulation between respiratory acquisition of infection compared with the bolus introduction of S-encoding mRNA or adenovirus following intramuscular vaccination. Nonetheless, the kinetics of recall of immune memory in SARS-CoV-2 is broadly consistent with studies of human influenza infection (Nguyen et al., 2021; Rahil et al., 2020).

Previous studies show viral growth rates and peak viral loads are comparable between vaccinated and unvaccinated individuals following SARS-CoV-2 infection, although vaccinated subjects show a faster viral clearance after the peak (Chia et al., 2022; Kissler et al., 2021). A major question is to identify which immune responses mediate rapid viral clearance and if this is mechanistically linked to protection from severe infection in vaccinated subjects. Several lines of evidence suggest neutralizing antibody responses may play a major role in protection from severe disease. For example, early treatment of COVID-19 patients with potently neutralizing monoclonal antibody treatments significantly reduces the risk of progression to severe disease (Chen et al., 2021; Stadler et al., 2022; Weinreich et al., 2021). Protection is generally not observed following analogous administration of convalescent plasma, suggesting while antibodies alone appear sufficient to moderate disease severity, neutralization potency is likely a critical determinant (RECOVERY Collaborative Group, 2021; Joyner et al., 2021). Despite the non-trivial differences between recall of endogenous antibody and passive antibody therapy, the timing and magnitude of the increase in neutralizing antibody titers in breakthrough infection constitute a plausible modality for the reduced risk of severe disease observed in population studies of breakthrough infections (Tenforde et al., 2021). Specifically, we found that viral loads peaked about 1 day prior to the recall of antibody responses for Delta breakthrough infections. Studies of intranasal SARS-CoV-2 challenge after intramuscular vaccination of non-human primates (Francica et al., 2021; Gagne et al., 2021) indicate a temporal disconnect in recall kinetics between anatomical compartments, with both SARS-CoV-2-specific and non-specific IgG titers increasing in the bronchoalveolar lavage fluid prior to antibody recall in the serum, though this may reflect inflammation-induced exudation.

While systemic recall of T cell responses was variable and limited in the first 10 days, we cannot preclude T cell migration to the site of infection. Therefore, any contribution of T cells in mitigating disease severity of breakthrough infections requires investigation in larger cohorts, with particular attention paid to SARS-CoV-2-specific T cells in the respiratory tract which would be favorably localized to temper viral replication. The use of HLA-peptide tetramers to track frequencies and phenotype of S-specific T cells may provide further insights to the contribution

(C and D) (C) Frequencies of S-specific class-switched B cells (IgD^-CD19^+) and (D) antibody-secreting cells (ASCs, $CD20^{lo}CD71^+$ B cells) determined by flow cytometry.

(E–G) (E) Frequencies of AIM^+ (CD25, OX-40) S-specific $CD4^+$ Tmem cells ($CD3^+CD4^+CD8^-CD45RA^-CXCR5^-$), (F) AIM^+ $CD4^+$ cTFH cells ($CD3^+CD4^+CD8^-CD45RA^-CXCR5^+$) and (G) AIM^+ (CD69, CD137) S-specific $CD8^+$ Tmem cells ($CD3^+CD8^+CD4^-$non-naive) after stimulation with 5 μg/mL of SARS-CoV-2 S protein. (C–G) N = 8 participants for Delta (purple), N = 6 for Omicron (green).

See also Figure S3.

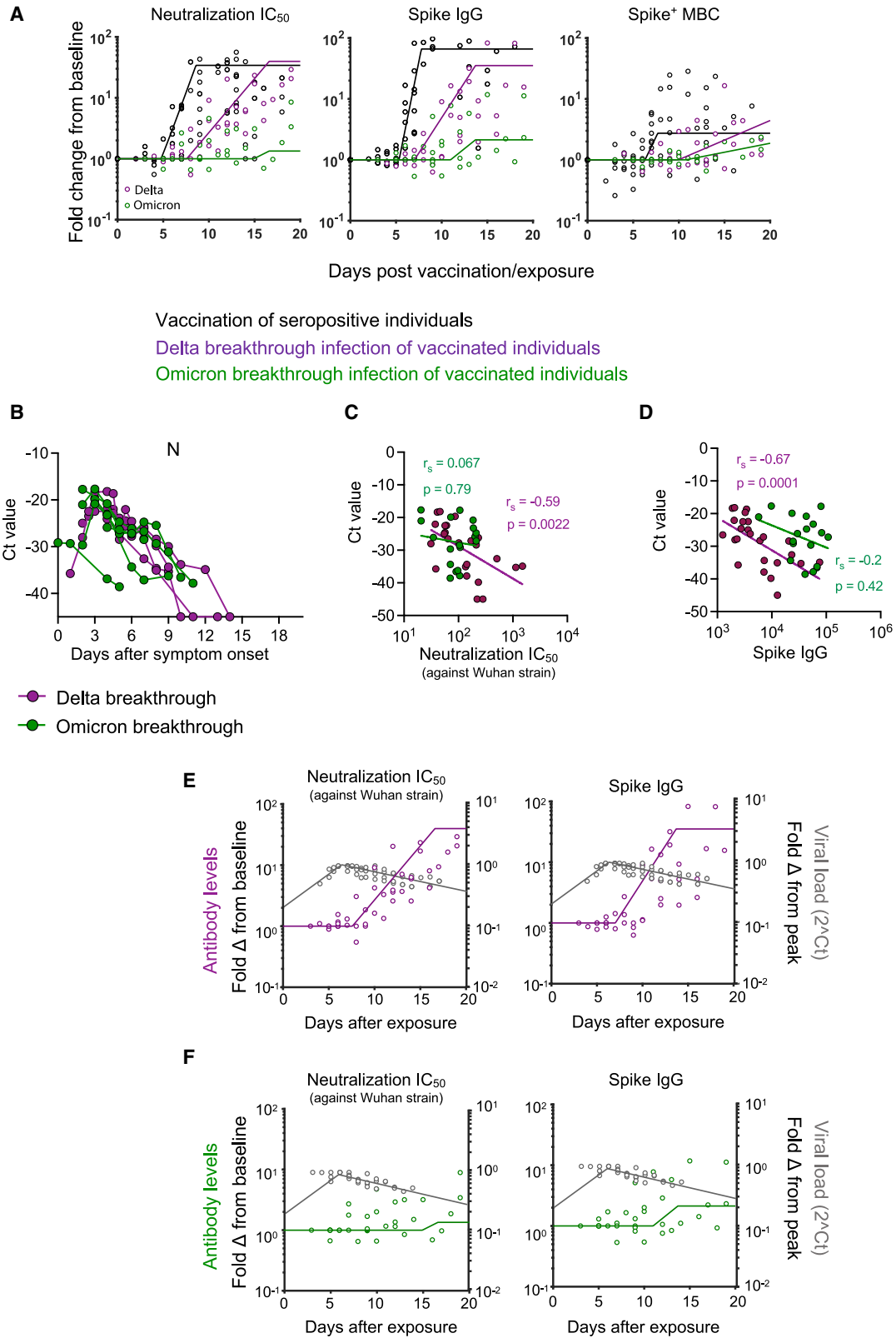

Figure 4. Immune recall following breakthrough infections is delayed compared with vaccination and preceded by peak viral load

(A) Comparative kinetics of immune recall following vaccination of seropositive individuals (black) and breakthrough infection of vaccinated individuals (Delta in purple, Omicron in green).

(legend continued on next page)

of T cells in the control of breakthrough infection (Wragg et al., 2022). Indeed, spike-specific $CD8^+$ T cells identified by class I dextramers show evidence of activation following either Delta or Omicron breakthrough infection at an average of day 10–11 post-infection, though the kinetics of such recall remains to be determined (Kared et al., 2022).

Encouragingly, we found breakthrough infection of vaccinated individuals with the Delta strain of SARS-CoV-2 reliably drove re-expansion of humoral immune memory with augmented neutralizing antibodies, albeit with some delay. This suggests that recall of immunity may plausibly contribute to the eventual mitigation of breakthrough disease severity. However, Omicron breakthrough infections, which generally have a milder clinical course (Nyberg et al., 2022), were markedly less capable of boosting prior responses to ancestral Hu-1 spike, in line with the extensive antigenic changes reported for this VOC (Cameroni et al., 2022). Therefore, while it seems breakthrough infection will play an important role in augmenting population level immunity against SARS-CoV-2, potentially reducing healthcare burdens and smoothing a pathway toward endemicity, this will be heavily influenced by the circulating viral strain and in particular, the degree of antigenic divergence from existing immune memory.

Limitations of the study

Some important caveats of our study include the significant age difference between the seronegative and the seropositive vaccinees and the lack of mucosal sampling of the upper or lower respiratory tracts. A major difficulty in studying the early kinetics of vaccine breakthrough infections has been rapid changes in (1) dominant viral strains in circulation and (2) vaccination status of the population over time. In this study, we collected breakthrough infections that covered the Delta to Omicron transition in Australia as well as the rollout of third dose boosters. This potentially confounds aspects of the study, where baseline distribution of boosters differed between the Delta (0 of 8) and Omicron (4 of 8) infections. Furthermore, the breakthrough infections studied to date have had favorable clinical outcomes, precluding meaningful analysis of immune recall stratified by disease severity. Expansion into larger cohorts will allow finer dissection of the drivers of breakthrough recall kinetics and magnitude.

STAR★METHODS

Detailed methods are provided in the online version of this paper and include the following:

- KEY RESOURCES TABLE
- RESOURCE AVAILABILITY
  - Lead contact
  - Materials availability
  - Data and code availability
- EXPERIMENTAL MODEL AND SUBJECT DETAILS
  - Human subjects
- METHOD DETAILS
  - ELISA
  - Microneutralization assay with ELISA-based readout
  - Flow cytometric detection of SARS-CoV-2-reactive B cells
  - Flow cytometric detection of antigen-specific T cells
  - Analysis of viral RNA load by qPCR
- QUANTIFICATION AND STATISTICAL ANALYSIS
  - Modelling the kinetics of immune recall

SUPPLEMENTAL INFORMATION

Supplemental information can be found online at https://doi.org/10.1016/j.immuni.2022.05.018.

ACKNOWLEDGMENTS

We thank the participants for the generous involvement and provision of samples. We thank T. Amarasena, R. Esterbauer, K. Wragg, P. Konstandopoulos, K. Field, and A. Kelly (University of Melbourne) for excellent technical assistance. We thank molecular staff at the Victorian Infectious Diseases Reference Laboratory for performing RT-PCR. We thank Dr. Julian Druce and Dr. Leon Caly at the Victorian Infectious Diseases Reference Laboratory for isolating and distributing SARS-CoV-2 virus isolates. We acknowledge the Melbourne Cytometry Platform for provision of flow cytometry services. This study was supported by the Australian National Health and Medical Research Council grants 1149990, 1162760, and 2004398; Australian Medical Research Future Fund grants 2005544 and 2013870; The Victorian Government; and Australian National Health and Medical Research Council Investigator or Fellowship grants (M.K., A.K.W., J.A.J., H.-X.T., D.A.W., M.P.D., and S.J.K.).

AUTHOR CONTRIBUTIONS

Conceptualization: M.K., W.S.L., A.K.W., J.A.J., M.P.D., S.J.K.; formal analysis: M.K., W.S.L., A.R., K.C.L., G.T., E.S., D.C., D.S.K., A.K.W., and J.A.J.; funding acquisition: A.K.W., J.A.J., M.P.D., and S.J.K.; investigation: M.K., W.S.L., A.R., H.-X.T., G.G., K.C.L., G.T., A.K.W., and J.A.J.; methodology: M.K., W.S.L., A.R., H.-X.T., G.G., K.C.L., A.K.W., and J.A.J.; resources: P.K., K.C.L., D.A.W., H.E.K., and S.J.K.; supervision: D.C., D.S.K., A.K.W., J.A.J., M.P.D., and S.J.K.; writing – original draft: M.K., W.S.L., A.K.W., J.A.J., M.P.D., and S.J.K.; writing – review & editing: M.K., W.S.L., A.R., H.-X.T., D.A.W., D.C., D.S.K., A.K.W., J.A.J., M.P.D., and S.J.K.

DECLARATION OF INTERESTS

The authors declare no competing interests.

Received: January 22, 2022
Revised: April 1, 2022
Accepted: May 23, 2022
Published: May 27, 2022

REFERENCES

Backer, J.A., Eggink, D., Andeweg, S.P., Veldhuijzen, I.K., van Maarseveen, N., Vermaas, K., Vlaemynck, B., Schepers, R., van den Hof, S., Reusken,

(B) Ct values for SARS-CoV-2 N gene in serial nasopharyngeal swabs. N = 4 participants for Delta, N = 7 for Omicron.
(C and D) Correlations between Ct value and titers of neutralizing antibodies (C) or spike IgG antibodies (D). Spearman correlation coefficients (r_s) and p values are indicated on the figure, n = 24 paired samples from 4 subjects for Delta and n = 18 paired samples from 7 subjects for Omicron.
(E and F) Overlayed kinetics of antibody recall (fold change over baseline) and viral load (fold change relative to peak) for neutralizing antibody titers and spike IgG antibodies for Delta (E) and Omicron (F) breakthrough infections.
(A, E, and F) The lines indicate the mean estimate for each group from the piecewise linear regression model using the estimated parameters.
See also Figure S4.

C.B., and Wallinga, J. (2022). Shorter serial intervals in SARS-CoV-2 cases with Omicron BA.1 variant compared with Delta variant, the Netherlands, 13 to 26 December 2021. Euro Surveill. *27*, 2200042. https://doi.org/10.2807/1560-7917.ES.2022.27.6.2200042.

Cameroni, E., Bowen, J.E., Rosen, L.E., Saliba, C., Zepeda, S.K., Culap, K., Pinto, D., VanBlargan, L.A., De Marco, A., di Iulio, J., et al. (2022). Broadly neutralizing antibodies overcome SARS-CoV-2 Omicron antigenic shift. Nature *602*, 664–670. https://doi.org/10.1038/s41586-021-04386-2.

Carreño, J.M., Alshammary, H., Tcheou, J., Singh, G., Raskin, A.J., Kawabata, H., Sominsky, L.A., Clark, J.J., Adelsberg, D.C., Bielak, D.A., et al. (2022). Activity of convalescent and vaccine serum against SARS-CoV-2 Omicron. Nature *602*, 682–688. https://doi.org/10.1038/s41586-022-04399-5.

Chan, J.F., Yip, C.C., To, K.K., Tang, T.H., Wong, S.C., Leung, K.H., Fung, A.Y., Ng, A.C., Zou, Z., Tsoi, H.W., et al. (2020). Improved molecular diagnosis of COVID-19 by the novel, highly sensitive and specific COVID-19-RdRp/Hel real-time reverse transcription-PCR assay validated *in vitro* and with clinical specimens. J. Clin. Microbiol. *58*, e00310–e00320. https://doi.org/10.1128/JCM.00310-20.

Chen, P., Nirula, A., Heller, B., Gottlieb, R.L., Boscia, J., Morris, J., Huhn, G., Cardona, J., Mocherla, B., Stosor, V., et al. (2021). SARS-CoV-2 neutralizing antibody LY-CoV555 in outpatients with Covid-19. N. Engl. J. Med. *384*, 229–237. https://doi.org/10.1056/NEJMoa2029849.

Chia, P.Y., Ong, S.W.X., Chiew, C.J., Ang, L.W., Chavatte, J.M., Mak, T.M., Cui, L., Kalimuddin, S., Chia, W.N., Tan, C.W., et al. (2022). Virological and serological kinetics of SARS-CoV-2 Delta variant vaccine breakthrough infections: a multicenter cohort study. Clin. Microbiol. Infect. *28*, 612.e1–612.e7. https://doi.org/10.1016/j.cmi.2021.11.010.

Chung, H., He, S., Nasreen, S., Sundaram, M.E., Buchan, S.A., Wilson, S.E., Chen, B., Calzavara, A., Fell, D.B., Austin, P.C., et al. (2021). Effectiveness of BNT162b2 and mRNA-1273 covid-19 vaccines against symptomatic SARS-CoV-2 infection and severe covid-19 outcomes in Ontario, Canada: test negative design study. BMJ *374*, n1943. https://doi.org/10.1136/bmj.n1943.

Corman, V.M., Landt, O., Kaiser, M., Molenkamp, R., Meijer, A., Chu, D.K., Bleicker, T., Brünink, S., Schneider, J., Schmidt, M.L., et al. (2020). Detection of 2019 novel coronavirus (2019-nCoV) by real-time RT-PCR. Euro Surveill *25*, 2000045. https://doi.org/10.2807/1560-7917.ES.2020.25.3.2000045.

Cromer, D., Steain, M., Reynaldi, A., Schlub, T.E., Wheatley, A.K., Juno, J.A., Kent, S.J., Triccas, J.A., Khoury, D.S., and Davenport, M.P. (2022). Neutralising antibody titres as predictors of protection against SARS-CoV-2 variants and the impact of boosting: a meta-analysis. Lancet Microbe *3*, e52–e61. https://doi.org/10.1016/S2666-5247(21)00267-6.

Ellebedy, A.H., Jackson, K.J., Kissick, H.T., Nakaya, H.I., Davis, C.W., Roskin, K.M., McElroy, A.K., Oshansky, C.M., Elbein, R., Thomas, S., et al. (2016). Defining antigen-specific plasmablast and memory B cell subsets in human blood after viral infection or vaccination. Nat. Immunol. *17*, 1226–1234. https://doi.org/10.1038/ni.3533.

Ferdinands, J.M., Thompson, M.G., Blanton, L., Spencer, S., Grant, L., and Fry, A.M. (2021). Does influenza vaccination attenuate the severity of breakthrough infections? A narrative review and recommendations for further research. Vaccine *39*, 3678–3695. https://doi.org/10.1016/j.vaccine.2021.05.011.

Francica, J.R., Flynn, B.J., Foulds, K.E., Noe, A.T., Werner, A.P., Moore, I.N., Gagne, M., Johnston, T.S., Tucker, C., Davis, R.L., et al. (2021). Protective antibodies elicited by SARS-CoV-2 spike protein vaccination are boosted in the lung after challenge in nonhuman primates. Sci. Transl. Med. *13*, eabi4547. https://doi.org/10.1126/scitranslmed.abi4547.

Gagne, M., Corbett, K.S., Flynn, B.J., Foulds, K.E., Wagner, D.A., Andrew, S.F., Todd, J.-P.M., Honeycutt, C.C., McCormick, L., Nurmukhambetova, S.T., et al. (2021). Protection from SARS-CoV-2 Delta one year after mRNA-1273 vaccination in rhesus macaques is coincident with anamnestic antibody response in the lung. Cell *185*, 113.e15. 130.e15. https://doi.org/10.1016/j.cell.2021.12.002.

Gilbert, P.B., Montefiori, D.C., McDermott, A.B., Fong, Y., Benkeser, D., Deng, W., Zhou, H., Houchens, C.R., Martins, K., Jayashankar, L., et al. (2021). Immune correlates analysis of the mRNA-1273 COVID-19 vaccine efficacy clinical trial. Science *375*, 43–50.

Joyner, M.J., Carter, R.E., Senefeld, J.W., Klassen, S.A., Mills, J.R., Johnson, P.W., Theel, E.S., Wiggins, C.C., Bruno, K.A., Klompas, A.M., et al. (2021). Convalescent plasma antibody levels and the risk of death from Covid-19. N. Engl. J. Med. *384*, 1015–1027. https://doi.org/10.1056/NEJMoa2031893.

Juno, J.A., Tan, H.X., Lee, W.S., Reynaldi, A., Kelly, H.G., Wragg, K., Esterbauer, R., Kent, H.E., Batten, C.J., Mordant, F.L., et al. (2020). Humoral and circulating follicular helper T cell responses in recovered patients with COVID-19. Nat. Med. *26*, 1428–1434. https://doi.org/10.1038/s41591-020-0995-0.

Kared, H., Wolf, A.-S., Alirezaylavasani, A., Ravussin, A., Solum, G., Tran, T.T., Lund-Johansen, F., Vaage, J.T., Nissen-Meyer, L.S., Nygaard, U.C., et al. (2022). Immunity in Omicron SARS-CoV-2 breakthrough COVID-19 in vaccinated adults. Preprint at medRxiv. https://doi.org/10.1101/2022.01.13.22269213.

Khoury, D.S., Cromer, D., Reynaldi, A., Schlub, T.E., Wheatley, A.K., Juno, J.A., Subbarao, K., Kent, S.J., Triccas, J.A., and Davenport, M.P. (2021). Neutralizing antibody levels are highly predictive of immune protection from symptomatic SARS-CoV-2 infection. Nat. Med. *27*, 1205–1211. https://doi.org/10.1038/s41591-021-01377-8.

Kissler, S.M., Fauver, J.R., Mack, C., Tai, C.G., Breban, M.I., Watkins, A.E., Samant, R.M., Anderson, D.J., Metti, J., Khullar, G., et al. (2021). Viral dynamics of SARS-CoV-2 variants in vaccinated and unvaccinated persons. N. Engl. J. Med. *385*, 2489–2491. https://doi.org/10.1056/NEJMc2102507.

Koutsakos, M., Lee, W.S., Wheatley, A.K., Kent, S.J., and Juno, J.A. (2022). T follicular helper cells in the humoral immune response to SARS-CoV-2 infection and vaccination. J. Leukoc. Biol. *111*, 355–365. https://doi.org/10.1002/JLB.5MR0821-464R.

Nguyen, T.H.O., Koutsakos, M., van de Sandt, C.E., Crawford, J.C., Loh, L., Sant, S., Grzelak, L., Allen, E.K., Brahm, T., Clemens, E.B., et al. (2021). Immune cellular networks underlying recovery from influenza virus infection in acute hospitalized patients. Nat. Commun. *12*, 2691. https://doi.org/10.1038/s41467-021-23018-x.

Nyberg, T., Ferguson, N.M., Nash, S.G., Webster, H.H., Flaxman, S., Andrews, N., Hinsley, W., Bernal, J.L., Kall, M., Bhatt, S., et al. (2022). Comparative analysis of the risks of hospitalisation and death associated with SARS-CoV-2 omicron (B.1.1.529) and delta (B.1.617.2) variants in England: a cohort study. Lancet *399*, 1303–1312. https://doi.org/10.1016/S0140-6736(22)00462-7.

Patel, M.M., York, I.A., Monto, A.S., Thompson, M.G., and Fry, A.M. (2021). Immune-mediated attenuation of influenza illness after infection: opportunities and challenges. Lancet Microbe *2*, e715. https://doi.org/10.1016/S2666-5247(21)00180-4.

Rahil, Z., Leylek, R., Schürch, C.M., Chen, H., Bjornson-Hooper, Z., Christensen, S.R., Gherardini, P.F., Bhate, S.S., Spitzer, M.H., Fragiadakis, G.K., et al. (2020). Landscape of coordinated immune responses to H1N1 challenge in humans. J. Clin. Invest. *130*, 5800–5816. https://doi.org/10.1172/JCI137265.

RECOVERY Collaborative Group (2021). Convalescent plasma in patients admitted to hospital with COVID-19 (RECOVERY): a randomised controlled, open-label, platform trial. Lancet *397*, 2049–2059. https://doi.org/10.1016/S0140-6736(21)00897-7.

Roessler, A., Riepler, L., Bante, D., von Laer, D., and Kimpel, J. (2021). SARS-CoV-2 B.1.1.529 variant (Omicron) evades neutralization by sera from vaccinated and convalescent individuals. N. Engl. J. Med. *386*, 698–700. https://doi.org/10.1056/NEJMc2119236.

Sahin, U., Muik, A., Vogler, I., Derhovanessian, E., Kranz, L.M., Vormehr, M., Quandt, J., Bidmon, N., Ulges, A., Baum, A., et al. (2021). BNT162b2 vaccine induces neutralizing antibodies and poly-specific T cells in humans. Nature *595*, 572–577. https://doi.org/10.1038/s41586-021-03653-6.

Shamier, M.C., Tostmann, A., Bogers, S., de Wilde, J., Ijpelaar, J., van der Kleij, W.A., de Jager, H., Haagmans, B.L., Molenkamp, R., Oude Munnink, B.B., et al. (2021). Virological characteristics of SARS-CoV-2 vaccine breakthrough infections in health care workers. Preprint at medRxiv. https://doi.org/10.1101/2021.08.20.21262158.

Singanayagam, A., Hakki, S., Dunning, J., Madon, K.J., Crone, M.A., Koycheva, A., Derqui-Fernandez, N., Barnett, J.L., Whitfield, M.G., Varro, R., et al. (2022). Community transmission and viral load kinetics of the SARS-CoV-2 delta (B.1.617.2) variant in vaccinated and unvaccinated individuals in the UK: a prospective, longitudinal, cohort study. Lancet Infect. Dis. *22*, 183–195. https://doi.org/10.1016/S1473-3099(21)00648-4.

Stadler, E., Chai, K.L., Schlub, T.E., Cromer, D., Polizzotto, M.N., Kent, S.J., Skoetz, N., Estcourt, L., McQuilten, Z.K., Wood, E.M., et al. (2022). Determinants of passive antibody effectiveness in SARS-CoV-2 infection. Preprint at medRxiv. https://doi.org/10.1101/2022.03.21.22272672.

Tang, P., Hasan, M.R., Chemaitelly, H., Yassine, H.M., Benslimane, F.M., Al Khatib, H.A., AlMukdad, S., Coyle, P., Ayoub, H.H., Al Kanaani, Z., et al. (2021). BNT162b2 and mRNA-1273 COVID-19 vaccine effectiveness against the SARS-CoV-2 Delta variant in Qatar. Nat. Med. *27*, 2136–2143. https://doi.org/10.1038/s41591-021-01583-4.

Tenforde, M.W., Self, W.H., Adams, K., Gaglani, M., Ginde, A.A., McNeal, T., Ghamande, S., Douin, D.J., Talbot, H.K., Casey, J.D., et al. (2021). Association between mRNA vaccination and COVID-19 hospitalization and disease severity. JAMA *326*, 2043–2054. https://doi.org/10.1001/jama.2021.19499.

Weinreich, D.M., Sivapalasingam, S., Norton, T., Ali, S., Gao, H., Bhore, R., Musser, B.J., Soo, Y., Rofail, D., Im, J., et al. (2021). REGN-COV2, a neutralizing antibody cocktail, in outpatients with Covid-19. N. Engl. J. Med. *384*, 238–251. https://doi.org/10.1056/NEJMoa2035002.

Wheatley, A.K., Juno, J.A., Wang, J.J., Selva, K.J., Reynaldi, A., Tan, H.X., Lee, W.S., Wragg, K.M., Kelly, H.G., Esterbauer, R., et al. (2021a). Evolution of immune responses to SARS-CoV-2 in mild-moderate COVID-19. Nat. Commun. *12*, 1162. https://doi.org/10.1038/s41467-021-21444-5.

Wheatley, A.K., Pymm, P., Esterbauer, R., Dietrich, M.H., Lee, W.S., Drew, D., Kelly, H.G., Chan, L.J., Mordant, F.L., Black, K.A., et al. (2021b). Landscape of human antibody recognition of the SARS-CoV-2 receptor binding domain. Cell Rep. *37*, 109822. https://doi.org/10.1016/j.celrep.2021.109822.

Wragg, K.M., Lee, W.S., Koutsakos, M., Tan, H.X., Amarasena, T., Reynaldi, A., Gare, G., Konstandopoulos, P., Field, K.R., Esterbauer, R., et al. (2022). Establishment and recall of SARS-CoV-2 spike epitope-specific CD4+ T cell memory. Nat. Immunol. *23*, 768–780. https://doi.org/10.1038/s41590-022-01175-5.

STAR★METHODS

KEY RESOURCES TABLE

REAGENT or RESOURCE	SOURCE	IDENTIFIER
Antibodies		
HRP-conjugated rabbit anti-human IgG	Agilent	Cat#P021402-2
Rabbit anti SARS-CoV N antibody	Rockland	Cat#200-401-A50
Trypsin TPCK	Fisher Scientific	Cat#NC9783694
CD19 J4.119 ECD	Beckman Coulter	Cat#IM2708U; RRID:AB_130854
IgD poly AF488	Southern Biotech	Cat#2030-30; RRID:AB_2795631
Streptavidin BV510	BD Biosciences	Cat#563261
CD20 2H7 APC-Cy7	BioLegend	Cat#302314; RRID:AB_314262
CD14 M5E2 BV510	BioLegend	Cat#301841; RRID:AB_2561379
CD8a RPA-T8 BV510	BioLegend	Cat#301048; RRID:AB_2561942
CD16 3G8 BV510	BioLegend	Cat#302048; RRID:AB_2562085
CD10 HI10a BV510	BioLegend	Cat#312220; RRID:AB_2563835
CD71 CY1G4 PeCy7	BioLegend	Cat#334112; RRID:AB_2563119
Streptavidin PE	Thermo Fisher Scientific	Cat#S866
CD69 FN50 FITC	BioLegend	Cat#310904; RRID:AB_314839
OX-40 ACT35 PerCP-Cy5.5	BioLegend	Cat#350010; RRID:AB_10719224
CD25 BC96 APC	BioLegend	Cat#302610; RRID:AB_314280
CCR7 150503 AF700	BD Biosciences	Cat#561143; RRID:AB_10562031
CD137 4B4-1 BV421	BioLegend	Cat#309820; RRID:AB_2563830
CD4 RPA-T4 BV605	BioLegend	Cat#300556; RRID:AB_2564391
CD8 RPA-T8 BV650	BioLegend	Cat#301042; RRID:AB_2563505
CXCR5 MU5UBEE PE	ThermoFisher	Cat#12-9185-42; RRID:AB_11219877
CD45RA HI100 PE-Cy7	BD Biosciences	Cat#560675; RRID:AB_1727498
CD3 SK7 BUV395	BD Biosciences	Cat#564000; RRID:AB_2744382
Bacterial and virus strains		
SARS-CoV-2 (CoV/Australia/VIC/01/2020)	Victorian Infectious Diseases Reference Laboratory	N/A
Biological samples		
Whole blood samples and derivatives (peripheral bloodmononuclear cells (PBMCs), plasma and serum) fromuninfected controls, COVID-19 convalescent donors and COVID-19 vaccinated subjects	The University of Melbourne	N/A
Chemicals, peptides, and recombinant proteins		
Recombinant SARS-CoV-2 spike protein	The University of Melbourne	In house
Recombinant SARS-CoV-2 RBD protein	The University of Melbourne	In house
TMB substrate	Sigma	Cat#T0440-1L
Deposited data		
Longitudinal data for HLA-DRB1*15/S_{751} tetramer-specific CD4+ T cells	Wragg et al., 2022	N/A
Experimental models: Cell lines		
Vero cells	Victorian Infectious Disease Reference Laboratory	N/A
Software and algorithms		
FlowJo v10	Tree Star	https://www.flowjo.com/
GraphPad Prism v8	GraphPad	https://www.graphpad.com/
Monolix	Lixoft	https://lixoft.com/products/monolix/

RESOURCE AVAILABILITY

Lead contact

Further information and requests for resources and reagents should be directed to and will be fulfilled by the lead contact, Stephen Kent (skent@unimelb.edu.au).

Materials availability

This study did not generate new unique reagents.

Data and code availability

- All data reported in this paper will be shared by the lead contact upon request.
- This study did not generate any unique datasets or code.
- Any additional information required to reanalyze the data reported in this paper is available from the lead contact upon request.

EXPERIMENTAL MODEL AND SUBJECT DETAILS

Human subjects

A cohort of subjects with either a prior positive nasal PCR for SARS-CoV-2 or a positive ELISA for SARS-CoV-2 S and RBD protein were recruited to provide blood samples following vaccination against SARS-CoV-2. Contemporaneous controls who had not previously experienced any symptoms of COVID-19 and who were confirmed to be seronegative were also recruited to provide blood samples prior to and following vaccination for SARS-CoV-2 (Table S1). A cohort of previously vaccinated participants with a nasal PCR-confirmed breakthrough COVID-19 were recruited through contacts with the investigators and invited to provide serial blood samples (Table S3). Individuals who reported a positive PCR and/or rapid antigen test within the past 35 days were invited to provide up to 2 samples for serological analysis. For all participants, whole blood was collected with sodium heparin anticoagulant. Plasma was collected and stored at -80°C, and PBMCs were isolated via Ficoll-Paque separation, cryopreserved in 10% DMSO/FCS and stored in liquid nitrogen.

The study protocols were approved by the University of Melbourne Human Research Ethics Committee (2021-21198-15398-3, 2056689), and all associated procedures were carried out in accordance with approved guidelines. All participants provided written informed consent in accordance with the Declaration of Helsinki.

METHOD DETAILS

ELISA

Antibody binding to SARS-CoV-2 S or RBD proteins was tested by ELISA. The expression of recombinant S and RBD has been described previously (Juno et al., 2020). For ELISA, 96-well Maxisorp plates (Thermo Fisher) were coated overnight at 4°C with 2 μg/ml recombinant S or RBD proteins. After blocking with 1% FCS in phosphate-buffered saline (PBS), duplicate wells of serially diluted plasma were added and incubated for 2 h at room temperature. Plates were washed in PBS-T (0.05% Tween-20 in PBS) and PBS before incubation with 1:20,000 dilution of HRP-conjugated anti-human IgG (Sigma) for 1 h at room temperature. Plates were washed and developed using TMB substrate (Sigma), stopped using sulphuric acid and read at 450 nm. Endpoint titers were calculated as the reciprocal serum dilution giving signal 2× background using a fitted curve (4 parameter log regression).

Microneutralization assay with ELISA-based readout

Plasma neutralization activity against SARS-CoV-2 was measured using a microneutralization assay as previously described (Wheatley et al., 2021b). Wildtype SARS-CoV-2 (CoV/Australia/VIC/01/2020) isolate was passaged in Vero cells and stored at -80°C. 96-well flat bottom plates were seeded with Vero cells (20,000 cells per well in 100μl). The next day, Vero cells were washed once with 200 μl serum-free DMEM and added with 150μl of infection media (serum-free DMEM with 1.33 μg/ml TPCK trypsin). 2.5-fold serial dilutions of heat-inactivated plasma (1:20-1:12207) were incubated with SARS-CoV-2 virus at 2000 $TCID_{50}$/ml at 37°C for 1 hour. Next, plasma-virus mixtures (50μl) were added to Vero cells in duplicate and incubated at 37°C for 48 hours. 'Cells only' and 'virus+cells' controls were included to represent 0% and 100% infectivity respectively. After 48 hours, all cell culture media were carefully removed from wells and 200 μl of 4% formaldehyde was added to fix the cells for 30 mins at room temperature. The plates were then dunked in a 1% formaldehyde bath for 30 minutes to inactivate any residual virus prior to removal from the BSL3 facility. Cells were washed once in PBS and then permeabilised with 150μl of 0.1% Triton-X for 15 minutes. Following one wash in PBS, wells were blocked with 200μl of blocking solution (4% BSA with 0.1% Tween-20) for 1 hour. After three washes in PBST (PBS with 0.05% Tween-20), wells were incubated with 100μl of rabbit polyclonal anti-SARS-CoV N antibody (Rockland, #200-401-A50) at a 1:8000 dilution in dilution buffer (PBS with 0.2% Tween-20, 0.1% BSA and 0.5% NP-40) for 1 hour. Plates were then washed six times in PBST and added with 100μl of goat anti-rabbit IgG (Abcam, #ab6721) at a 1:8000 dilution for 1 hour. After six washes in PBST, plates were developed with TMB and stopped with 0.15M H_2SO_4. OD values read at 450nm were then used to calculate %neutralization with the following formula: ('Virus + cells' – 'sample') ÷ ('Virus + cells' – 'Cells only') × 100. IC_{50} values were determined using

four-parameter nonlinear regression in GraphPad Prism with curve fits constrained to have a minimum of 0% and maximum of 100% neutralization.

Flow cytometric detection of SARS-CoV-2-reactive B cells

Probes for delineating SARS-CoV-2 S-specific B cells within cryopreserved human PBMCs were generated by sequential addition of streptavidin-phycoerythrin (PE) (Thermo Fisher) to trimeric S protein biotinylated using recombinant Bir-A (Avidity). Cells were stained with Aqua viability dye (Thermo Fisher) in PBS. Cells were then stained with S-PE probes and surface monoclonal antibodies in 1% FCS in PBS for 30 mins at 4°C. Monoclonal antibodies for surface staining included CD19-ECD (J3-119, 1:150) (Beckman Coulter), IgM BUV395 (G20-127, 1:150), CD21 BUV737 (B-ly4, 1:150), IgG BV786 (G18-145, 1:75), streptavidin-BV510 (1:600), CD11c (B-ly6, 1:100) (BD Biosciences), CD20 APC-Cy7 (2H7, 1:150), CD14 BV510 (M5E2, 1:300), CD3 BV510 (OKT3, 1:600), CD8a BV510 (RPA-T8, 1:1500), CD16 BV510 (3G8, 1:500), CD10 BV510 (HI10a, 1:750) and CD27 BV605 (O323, 1:150), CD71 PeCy7 (CY1G4, 1:100) (BioLegend), IgD AF488 (Goat polyclonal, 1:100) (Southern Biotech), IgA VioBlue (IS11-8E10, 1:100) (Miltenyi Biotec). Cells were washed, fixed with 1% formaldehyde (Polysciences) and acquired on a BD LSR Fortessa.

Flow cytometric detection of antigen-specific T cells

Analysis of SARS-CoV-2-specific T cells was performed as previously described (Juno et al., 2020). Briefly, cryopreserved human PBMCs were thawed and rested for 4 h at 37°C. Cells were cultured in 96-well plates at 0.5-4 × 10^6 cells per well and stimulated for 20 h with 5 μg ml^{-1} of protein (BSA, SARS-CoV-2 S). Cells from selected donors were also stimulated with SEB (5 μg ml^{-1}) as a positive control. An CD154 APC-Cy7 (TRAP-1, BD Biosciences) antibody was included in the culture medium for the duration of the stimulation. After stimulation, cells were washed, stained with Live/Dead blue viability dye (Thermo Fisher) and incubated in a cocktail of monoclonal antibodies: CD27 BV510 (L128, 1:50), CCR7 Alexa700 (150503, 1:50), CD45RA PE-Cy7 (HI100, 1:200), (BD Biosciences), CD3 BUV395 (SK7, 1:100), CD4 BV605 (RPA-T4, 1:100), CD8 BV650 (RPA-T8, 1:400), CD25 APC (BC96, 1:50), OX-40 PerCP-Cy5.5 (ACT35, 1:50), CCR6 BV785 (G034E3, 1:100), CXCR3 PE-Dazzle 594 (G02H57, 1:50), CD69 FITC (FN50, 1:200), CD137 BV421 (4B4-1, 1:100) (BioLegend) and CXCR5 PE (MU5UBEE, Thermo Fisher, 1:50). Cells were washed, fixed with 1% formaldehyde and acquired on a BD LSR Fortessa using BD FACS Diva.

The HLA-DRB1*15/S751 tetramer (ProImmune) and associated data are described in Wragg et al (Wragg et al., 2022). Briefly, cells were incubated with 50nM dasatinib for 30 minutes at 37°C, then stained with PE-conjugated tetramer at 4ug/mL for 60 minutes at 37°C. Cells were washed in PBS, labelled with Live/Dead green viability dye, and stained with a cocktail of surface antibodies for 30 minutes at 4°C. Surface stain antibodies included: CD45RA PerCP-Cy5.5 (HI100), CD4 BV605 (RPA-T4), CD3 BUV395 (SK7) and CD20 BUV805 (2H7) (BD Biosciences).

Analysis of viral RNA load by qPCR

Nucleic acid extraction and complementary DNA (cDNA) synthesis

For viral RNA extraction, 200 μL of sample was extracted with the QIAamp 96 Virus QIAcube HT kit (Qiagen, Germany) on the QIAcube HT System (Qiagen) according to manufacturer's instructions. Purified nucleic acid was then immediately converted to cDNA by reverse transcription with random hexamers using the SensiFAST cDNA Synthesis Kit (Bioline Reagents, UK) according to manufacturer's instructions. cDNA was used immediately in the rRT-PCR or stored at -20°C. Three microlitres of cDNA was added to a commercial real-time PCR master mix (PrecisionFast qPCR Master Mix; Primer Design, UK) in a 20 μL reaction mix containing primers and probe with a final concentration of 0.9 mM and 0.2 mM for each primer and the probe, respectively. Samples were tested for the presence of SARS-CoV-2 RNA-dependent RNA polymerase (RdRp)/helicase (Hel), spike (S), and nucleocapsid (N) genes using previously described primers and probes (Chan et al., 2020; Corman et al., 2020). Thermal cycling and rRT-PCR analyses for all assays were performed on the ABI 7500 FAST real-time PCR system (Applied Biosystems, USA) with the following thermal cycling profile: 95C for 2 min, followed by 45 PCR cycles of 95C for 5 s and 60C for 25 s for N gene and 95C for 2 min, followed by 45 PCR cycles of 95C for 5 s and 55C for 25 s for RdRP/Helicase gene and S gene.

QUANTIFICATION AND STATISTICAL ANALYSIS

Modelling the kinetics of immune recall

We used a piecewise linear regression model to estimate the activation time and growth rate of various immune responses after vaccination and breakthrough infection. The model of the immune response y for subject i at time y_i can be written as:

$$y_i(t) = \begin{cases} (B+b_i);\ t \geq T_1+\tau_{1i} \\ (B+b_i)e^{(G+g_i)(t-(T_1+\tau_{1i}))};\ T_1+\tau_{1i} \leq t < T_2+\tau_{2i} \\ (B+b_i)e^{(G+g_i)((T_2+\tau_{2i})-(T_1+\tau_{1i}))} \times e^{-(D+d_i)(t-(T_2+\tau_{2i}))};\ t \geq T_2+\tau_{2i}. \end{cases}$$

The model has 5 parameters: $\boldsymbol{B}, \boldsymbol{G}, \boldsymbol{T}_1, \boldsymbol{D}$, and $\boldsymbol{T}_2$. For a period before $\boldsymbol{T}_1$, we assumed a constant baseline value $\boldsymbol{B}$ for the immune response. After the activation time $\boldsymbol{T}_1$, the immune response will grow at a rate of $\boldsymbol{G}$ until $\boldsymbol{T}_2$. From $\boldsymbol{T}_2$, the immune response will decay at a rate of $\boldsymbol{D}$. For each subject $\boldsymbol{i}$, the parameters were taken from a normal distribution, with each parameter having its own mean (fixed effect). A diagonal random effect structure was used, where we assumed there was no correlation within the random effects. The model was fitted to the log-transformed data values, with a constant error model distributed around zero with a standard

deviation σ. To account for the values less than the limit of detection, a censored mixed effect regression was used to fit the model. Values less 20, 100, and 0.0001 were censored for the neutralization, IgG bindings, and T cell data respectively. A binary covariate was used to quantify the difference in parameters between different groups (i.e. Delta vs Omicron breakthrough infection), and significance was determined based on the value of this binary covariate using a Wald test. Delta breakthrough infections were further stratified by symptom severity (mild vs moderate), duration of symptoms (<5.5 days vs ≥ 5.5 days) and time since last vaccine dose (<3 months vs ≥ 3 months). Further subgroup analysis within omicron breakthrough infections was not possible due to limited recall of immune responses. Model fitting was performed using MonolixR2019b.